NASA Technical Memorandum 110426 USAATCOM Technical Report 96-A-012

Flow Field Around a Hovering Rotor

C. Tung and S. Low, *Aeroflightdynamics Directorate, U.S. Army Aviation and Troop Command, Ames Research Center, Moffett Field, California*

February 1997

National Aeronautics and
Space Administration

Ames Research Center
Moffett Field, CA 94035-1000

US Army
Aviation and Troop Command

Aeroflightdynamics Directorate
Moffett Field, CA 94035-1000

TABLE OF CONTENTS

SYMBOLS

c	chord of generator airfoil, m
Cd	drag coefficient
C_l	lift coefficient
C_m	quarter-chord pitching-moment coefficient
r	radial distance from the vortex center, m
Re	Reynolds number, $U_\infty C/\nu$
U_∞	free-stream velocity, m/sec
w	circumferential-velocity component, m/sec
α	airfoil incidence, deg
φ	azimuthal angle, deg
Γ	circulation
ν	kinematic viscosity, m^2/sec

FLOW FIELD AROUND A HOVERING ROTOR

C. TUNG AND S. LOW*

Aeroflightdynamics Directorate
U. S. Army, Aviation and Missile Command
Ames Research Center

SUMMARY

A lifting surface hover code developed by the Analytical Method Inc.(AMI) was used to compute the average and unsteady velocity flow field of an isolated rotor without ground effect. The predicted velocity field compares well with experimental data obtained by hot-wire anemometry and by Laser Doppler Velocimetry. A subroutine "DOWNWASH" was written to predict the velocity field at any given point in the wake for a given blade position.

INTRODUCTION

The flow field around a hovering rotor is very complex since the tip vortices are quite close to the blades. The flow field is also unsteady in nature. The accurate determination of the flow field is important when the helicopter is used as a weapon platform or requires store separation. The initial speed of a free-flight projectile such as a rocket or a fuel tank is about the same magnitude as the flow velocities. Hence, the flow field has a great impact on the rocket and store separation trajectory. The U. S. Army has sponsored several contracts to United Technologies Research Center in the seventies to investigatge the airflow characteristics in the vicinity of a model AH-1G helicopter operating in hover and low forward flight conditions as reported in reference 1. Laser velocimetry and flow visualization using smokes were used to provide flow velocity and wake geometry data for rocket trajectory analysis and correlation with a wake velocity prediction.

Recently, as a part of the SEEK EAGLE program, an effort was initiated to develop a computer program that can be used for clearance and fly out simulation to assist in the airworthiness qualification and certification process of weapons and other stores on tri-service rotary-wing aircraft (ref. 2). This analysis requires the flow field around the helicopter as an input in a tabulated format so the store trajectories can be calculated and displayed on the screen of a graphic terminal in real time. Therefore, a hover performance code HOVER (ref. 3) for an isolated rotor has been used to calculate

---

*Sterling Software
Ames Research Center
Moffett Field, California

the flow field around a N-bladed rotor with N = 2 to 8. In particular, the vertical component of the instantaneous velocity (downwash) for both 2- and 4-blade rotor was computed and compared with the test data.

The gross weight of each helicopter depends on the mission assignment. It is impractical to calculate the flow field of the same helicopter of different weight over and over again. Therefore, an analysis has since been extended to correlate the downwash velocity with the gross weight.

It is the purpose of this report to document the prediction methodology and compare the predicted wake velocity with available test data. However, the influence of various helicopter components such as fuselage, wing and tail-rotor has not been included.

DESCRIPTION OF THE CALCULATION

In the computer code HOVER, each rotor blade is represented by a lifting surface through the use of a vortex lattice. The actual blade section geometries and section aerodynamics from tables containing 2-D values for lift, drag, and moment coefficient as a function of Mach number and angle of attack are input at user defined stations along the blade radius. A typical rotor blade vortex lattice model is shown in figure 1. The rotor airloads are computed on the projected planform. The program allows a maximum number of six rows of panels across the chord and thirty columns across the radius. Boundary condition points are inposed at two midspan locations on each panel.

The overall wake structure consists of three parts, namely, near-, intermediate- and far-wake regions. The detailed structure in the near and intermediate wake is modeled by distrete vortex filaments. The far wake is represented by a semi-infinite continuation of the intermediate wake. The near-wake geometry can either be prescribed or be a free wake. For a prescribed wake, there are four options concerning the discrete vortex filaments in the near-wake region:

1. Kocurek/Tangler Wake (ref. 4),

2. Landgrebe Wake (ref. 5),

3. User Input Tip Wake Constants, and

4. User Input Tip and Inner Sheet Constants.

For a free wake, the complete wake, with the exception of the root vortex, is relaxed. However a vortex core model is required to compute the self-induced velocity.

The intermediate-wake region serves as a buffer zone between the near-wake and the far-wake models. No wake contraction is allowed in this region, so the wake filaments are represented by constant-radius and fixed-pitch vortex helices. The radius and pitch of each filament is determined by the final radius and pitch of the filament in the near wake. The details of the analysis and the input data for the HOVER code are presented in reference 3. The unsteady flow field around the rotor is a part of the output from the HOVER code.

COMPARISON WITH TEST DATA

There are only limited wake velocity measurements available. Three different tests (Refs. 6 to 8) which range from model-scale to full-scale rotor are selected for comparison.

In reference 6, the three-component wake velocity of a full-scale OH-13E helicopter rotor mounted on a 60-foot rotor test tower was measured by a split-film total vector anemometer. Both time-averaged and instantaneous velocity along wake radii at various distances below the rotor disk were measured at different disk loadings and rotor speeds. The test condition selected for comparison was V_{tip} = 192.4 m/sec, C_T = 0.0021 and z/R = -0.1. figures 2(a) to 2(d) show good comparison of predicted instantaneous velocities at four different azimuthal angles (for $\varphi = 0^\circ, 45^\circ, 90^\circ$, and 135°) with measurements. The azimuthal angle φ is measured from a given blade. It is well known that the induced velocity increases as the radial distance approaches the center of the vortex. As seen in figures 2(b) and 2(c), the trailing vortex is located about eighty two percent of the rotor radius. The induced velocity due to the tip vortex adds to the induced velocity from the rest of the wake as approaching the tip vortex from inboard to outboard. After passing the center of the vortex, the induced velocity from the tip vortex substracts.The high velocity region depends on the location of measurements and calculations. Figure 2(b) indicates the calculation point is closer to the vortex core than the measurement points, thus the predicted velocity is higher than the measurements. While in figure 2(c), the measurement point is closer to the center of the vortex and has a higher velocity. The mean value of the velocity flow field is shown in figure 3. The prediction of the averaged velocity by the HOVER code agrees well with test data.

The second set of test data (ref. 7) was obtained from the downwash measuremeants of three-component velocity using hot-wire probes in an X-configuration. The four-blade hingeless rotor has a diameter of four meters, a linear four degrees of twist and a NACA-23012 airfoil. Figures 4 and 5 show the three components of the velocity at a distance of seven and thirty percent of the radius below the rotor blade respectively. In figure 4, the peak value for each velocity component is located around r/R = 0.9. This implies that the tip vortex is located at the ninety percent radial station for z/R = -0.07. The tip vortex moves inboard to around r/R = 0.8 for z/R = -0.3 by the same reason. The comparison of each velocity component with test data is reasonable.

Figures 6(a) to 6(f) show the comparison of predictions with measured results at six different azimuthal angles (ref. 8) at a distance about eighteen percent radius below the rotor plan. The test was conducted on a four-blade model rotor using an Laser Doppler Velocimetry system for velocity measurements. The solid line is the measurement and the dash line indicates the prediction. Again, the agreement is very good.

APPLICATION

The verification of AMI's HOVER code gives us the confidence to use this code for predicting the rotor downwash velocity. A typical run for the AH-64 Apache helicopter with 6480 kg weight in hover is given in Appendix A. The output consists of hover performance data such as thrust coefficient, power coefficient and three components of velocity for three different planes below the

rotor (z/R = -0.1, -0.3, -0.5 respectively) and every 30° azimuthal angle increment. All the velocities are normalized by the main rotor tip velocity of 221 m/sec. For an AH-64 Apache of non-standard weight, an empirical formula for the downwash is given in Appenix B.

It is impractical to use the HOVER code to calculate the rotor downwash for real-time simulation. Therefore, a separate subroutine call "DOWNWASH" was written to interpolate the velocity field output from the HOVER code in order to compute the downwash along a rocket trajectory. This subroutine is of the stand alone type and can be used in any trajectory simulation. The FORTRAN source code for the subroutine DOWNWASH is given in Appendix C.

CONCLUDING REMARKS

To predict a store separation or rocket trajectory released from a helicopter under the influence of a rotor wake requires accurate knowledge of the velocity flow field. The AMI HOVER code can be used for predicting the flow field. The code was validated by comparing with measurements obtained from a model rotor test to a full scale whirl tower test. The flow field of an AH-64 Apache was calculated as an example. Gross weights differing from the standard may be scaled by the weight ratio raised to the 0.454 power. It is noted that the flow field of any helicopter other than the AH-64 Apache should be calculated again using the HOVER code.

REFERENCES

1. Taylor, R. B. and Landgrebe, A. J.: Investigation of the Airflow at Rocket Trajectory and Wind Sensor Locations of a Model Helicopter Simulating Low Speed Flight. UTRC Report No. R79-912985-5, September, 1979.

2. Hall, B. H., Jr. and Robinson, C. E.: Demonstration of the Simulation and Visualization of Store Separation from Rotary Winged Aircraft. AEDC-TMR-92-P1, January, 1992.

3. Summa, J. M.: A Lifting-surface Method for Hover/Climb Airloads. Presented at the 35th Annual Forum of the American Helicopter Society, Washington D. C., May, 1979.

4. Kocurek, J. D., and Tangler, J. L.: Prescribed Wake Lifting Surface Hover Performance Analysis. Presented at the 32nd Annual Forum of the American Helicopter Society, Washington, D. C., May 1976.

5. Landgrebe, A. J.: An Analytical and Experimental Investigation of Helicopter Rotor Hover Performance and Wake Geometry Characteristics. USAAMRDL TR-71-24, June, 1971.

6. Boatwright, D. W.: Measurements of Velocity Components in the Wake of a Full-Scale Helicopter Rotor in Hover. USAAMRDL TR-72-33, August 1972.

7. Junker, B., and Langer, H.-J.: Helicopter Rotor Downwash Results of Experimental Research and comparison with Some Theoretical Results. Vertica, vol. 7, no. 1, pp. 61–70, 1983.

8. Nsi-Mba, M.: Contribution a l'Etude Experimentale et Numerique de l'Aerodyna-mique d'une Voilure Tournante. Thesis No. 207.208.89.46, Istitut de Mechanique des Fluides de Marseille, Universite d'Aix Marseille II, September, 1989.

APPENDIX A

USER INPUT

APACHE AH-64 ROTOR

NUMBER OF ROWS(CHORDWISE ELEMENTS) = 6

NUMBER OF COLUMNS(RADIAL ELEMENTS) = 15

NUMBER OF INPUT SECTIONS = 6

NUMBER OF ELEMENTS = 90

NUMBER OF LATTICE POINTS = 112

MAXIMUM OF BC POINTS = 105

NUMBER OF STRIPS IN EACH SECTION

2 3 2 6 2

INPUT PERFORMANCE DATA

BLADES	RADIUS	VTIP	VCLIMB	VSOUND	DENSITY	THRUST	COLLECTIVE
4			0.00	1155.00		7.50	
	24.00	725.00			0.002380		0.007000

RPM = 288.47

ROTOR PARAMETRIC INFORMATION

NC	YBC	MACH	TWIST	SWEEP	DYVL	CHORD	XC4	CLA
1	0.225	0.141	4.61	0.00	0.050000	0.062500	0.000000	0.120740
2	0.275	0.173	3.94	0.00	0.050000	0.062500	0.000000	0.121351
3	0.350	0.220	3.22	0.00	0.100000	0.062500	0.000000	0.122523
4	0.450	0.282	2.47	0.00	0.100000	0.062500	0.000000	0.124604
5	0.550	0.345	1.72	0.00	0.100000	0.062500	0.000000	0.127360
6	0.650	0.408	0.90	0.00	0.100000	0.062500	0.000000	0.130923
7	0.750	0.471	0.00	0.00	0.100000	0.062500	0.000000	0.135482
8	0.815	0.512	-0.58	0.00	0.030000	0.062500	0.000000	0.139111

ROTOR PARAMETRIC INFORMATION (continued)

NC	YBC	MACH	TWIST	SWEEP	DYVL	CHORD	XC4	CLA
9	0.845	0.530	-0.86	0.00	0.030000	0.062500	0.000000	0.140998
10	0.875	0.549	-1.13	0.00	0.030000	0.062500	0.000000	0.143035
11	0.905	0.568	-1.40	0.00	0.030000	0.062500	0.000000	0.145240
12	0.935	0.587	-1.67	0.00	0.030000	0.062500	0.000000	0.147630
13	0.965	0.606	-1.94	0.00	0.030000	0.062500	0.000000	0.150226
14	0.984	0.618	-2.11	0.00	0.008889	0.062500	0.000000	0.152030
15	0.993	0.624	-2.19	0.00	0.008889	0.062500	0.000000	0.152889

RESULTANT SECTIONAL LOADS(LIFTING SURFACE CALCULATIONS)

I	Y	M	ALPHA	ALPI	CIRC	CTI	CXI	CQI	CLI	
1	0.225	0.141	7.33	4.78	0.520E-02	0.372E-03	0.311E-04	0.700E-05	0.741663	0.061870
2	0.275	0.173	6.34	5.09	0.619E-02	0.542E-03	0.483E-04	0.133E-04	0.723064	0.064278
3	0.350	0.220	5.74	4.99	0.713E-02	0.795E-03	0.694E-04	0.243E-04	0.654693	0.057012
4	0.450	0.282	5.19	4.79	0.839E-02	0.120E-02	0.101E-03	0.453E-04	0.598955	0.050025
5	0.550	0.345	4.77	4.45	0.960E-02	0.168E-02	0.131E-03	0.720E-04	0.560230	0.043537
6	0.650	0.408	4.36	4.04	0.106E-01	0.220E-02	0.155E-03	0.101E-03	0.523870	0.036914
7	0.750	0.471	3.91	3.59	0.113E-01	0.270E-02	0.170E-03	0.127E-03	0.483484	0.030314
8	0.815	0.512	3.56	3.35	0.116E-01	0.300E-02	0.176E-03	0.143E-03	0.455456	0.026631
9	0.845	0.530	3.40	3.25	0.118E-01	0.317E-02	0.180E-03	0.152E-03	0.447503	0.025349
10	0.875	0.549	3.31	3.07	0.122E-01	0.341E-02	0.183E-03	0.160E-03	0.448268	0.023993
11	0.905	0.568	3.66	2.44	0.131E-01	0.379E-02	0.162E-03	0.146E-03	0.465170	0.019842
12	0.935	0.587	4.15	1.68	0.135E-01	0.401E-02	0.118E-03	0.110E-03	0.461298	0.013538
13	0.965	0.606	3.90	1.66	0.118E-01	0.363E-02	0.105E-03	0.102E-03	0.392416	0.011380
14	0.984	0.618	3.46	1.93	0.882E-02	0.276E-02	0.932E-04	0.917E-04	0.286923	0.009668
15	0.993	0.624	3.17	2.14	0.579E-02	0.183E-02	0.685E-04	0.681E-04	0.186662	0.006984

THRUST COEFFICIENT = 0.62976E-02 THRUST COEFFICIENT PER SOLIDITY = 0.79138E-01

INDUCED TORQUE COEFFICIENT = 0.25510E-03 INDUCED TORQUE COEFFICIENT PER

SOLIDITY = 0.32057E-02

WAKE VELOCITY GRID PLANE INPUT BOUNDARIES

(NPL, PHI1, PHI2)

13 0.0000 90.0000

(NRL, R1, R2)

15 0.3000 1.0000

(NZL, Z1, Z2)

3 -0.1000 -0.5000

GRID PLANE VELOCITIES

GRID PLANE 1 AZIMUTH ANGLE = 0.00

N	R	X	Y	Z	VX	VY	VZ	VR	VT	V
1	0.300	0.300	0.000	-0.100	0.012	-0.280	-0.035	0.012	-0.280	0.282
2	0.300	0.300	0.000	-0.300	-0.001	-0.284	-0.039	-0.001	-0.284	0.287
3	0.300	0.300	0.000	-0.500	-0.003	-0.284	-0.046	-0.003	-0.284	0.288
4	0.350	0.350	0.000	-0.100	0.005	-0.330	-0.036	0.005	-0.330	0.332
5	0.350	0.350	0.000	-0.300	-0.002	-0.335	-0.044	-0.002	-0.335	0.338
6	0.350	0.350	0.000	-0.500	0.000	-0.336	-0.050	0.000	-0.336	0.339
7	0.400	0.400	0.000	-0.100	0.001	-0.379	-0.043	0.001	-0.379	0.382
8	0.400	0.400	0.000	-0.300	-0.002	-0.386	-0.050	-0.002	-0.386	0.389
9	0.400	0.400	0.000	-0.500	-0.002	-0.386	-0.058	-0.002	-0.386	0.391
10	0.450	0.450	0.000	-0.100	-0.005	-0.430	-0.040	-0.005	-0.430	0.432
11	0.450	0.450	0.000	-0.300	0.003	-0.435	-0.064	0.003	-0.435	0.439
12	0.450	0.450	0.000	-0.500	-0.002	-0.437	-0.065	-0.002	-0.437	0.442
13	0.500	0.500	0.000	-0.100	-0.005	-0.478	-0.051	-0.005	-0.478	0.481
14	0.500	0.500	0.000	-0.300	-0.006	-0.486	-0.064	-0.006	-0.486	0.490
15	0.500	0.500	0.000	-0.500	-0.005	-0.489	-0.059	-0.005	-0.489	0.493
16	0.550	0.550	0.000	-0.100	-0.001	-0.531	-0.034	-0.001	-0.531	0.532
17	0.550	0.550	0.000	-0.300	-0.009	-0.536	-0.068	-0.009	-0.536	0.541
18	0.550	0.550	0.000	-0.500	-0.006	-0.537	-0.079	-0.006	-0.537	0.543
19	0.600	0.600	0.000	-0.100	-0.010	-0.578	-0.056	-0.010	-0.578	0.581
20	0.600	0.600	0.000	-0.300	-0.014	-0.587	-0.070	-0.014	-0.587	0.591
21	0.600	0.600	0.000	-0.500	-0.007	-0.588	-0.080	-0.007	-0.588	0.594
22	0.650	0.650	0.000	-0.100	-0.010	-0.628	-0.059	-0.010	-0.628	0.630
23	0.650	0.650	0.000	-0.300	-0.013	-0.637	-0.075	-0.013	-0.637	0.642
24	0.650	0.650	0.000	-0.500	-0.009	-0.639	-0.081	-0.009	-0.639	0.644
25	0.700	0.700	0.000	-0.100	-0.018	-0.678	-0.060	-0.018	-0.678	0.680
26	0.700	0.700	0.000	-0.300	-0.009	-0.688	-0.078	-0.009	-0.688	0.692
27	0.700	0.700	0.000	-0.500	-0.012	-0.690	-0.081	-0.012	-0.690	0.694
28	0.750	0.750	0.000	-0.100	-0.021	-0.728	-0.062	-0.021	-0.728	0.731
29	0.750	0.750	0.000	-0.300	-0.013	-0.737	-0.088	-0.013	-0.737	0.743
30	0.750	0.750	0.000	-0.500	-0.001	-0.740	-0.085	-0.001	-0.740	0.745
31	0.800	0.800	0.000	-0.100	-0.026	-0.778	-0.064	-0.026	-0.778	0.781
32	0.800	0.800	0.000	-0.300	-0.044	-0.784	-0.121	-0.044	-0.784	0.795
33	0.800	0.800	0.000	-0.500	0.008	-0.795	-0.045	0.008	-0.795	0.797
34	0.850	0.850	0.000	-0.100	-0.024	-0.830	-0.057	-0.024	-0.830	0.832

GRID PLANE 1 AZIMUTH ANGLE = 0.00 (continued)

N	R	X	Y	Z	VX	VY	VZ	VR	VT	V
35	0.850	0.850	0.000	-0.300	-0.034	-0.850	0.028	-0.034	-0.850	0.851
36	0.850	0.850	0.000	-0.500	0.003	-0.850	-0.002	0.003	-0.850	0.850
37	0.900	0.900	0.000	-0.100	0.011	-0.885	-0.027	0.011	-0.885	0.886
38	0.900	0.900	0.000	-0.300	-0.004	-0.899	0.008	-0.004	-0.899	0.899
39	0.900	0.900	0.000	-0.500	-0.001	-0.900	0.005	-0.001	-0.900	0.900
40	0.950	0.950	0.000	-0.100	0.007	-0.940	0.011	0.007	-0.940	0.940
41	0.950	0.950	0.000	-0.300	-0.002	-0.949	0.007	-0.002	-0.949	0.949
42	0.950	0.950	0.000	-0.500	-0.002	-0.950	0.005	-0.002	-0.950	0.950
43	1.000	1.000	0.000	-0.100	-0.002	-0.993	0.013	-0.002	-0.993	0.994
44	1.000	1.000	0.000	-0.300	-0.003	-0.999	0.007	-0.003	-0.999	0.999
45	1.000	1.000	0.000	-0.500	-0.002	-1.000	0.005	-0.002	-1.000	1.000

GRID PLANE 5 AZIMUTH ANGLE = 30.00

N	R	X	Y	Z	VX	VY	VZ	VR	VT	V
1	0.300	0.260	0.150	-0.100	0.155	-0.241	-0.039	0.014	-0.286	0.289
2	0.300	0.260	0.150	-0.300	0.145	-0.246	-0.038	0.002	-0.285	0.288
3	0.300	0.260	0.150	-0.500	0.140	-0.248	-0.042	-0.003	-0.285	0.288
4	0.350	0.303	0.175	-0.100	0.179	-0.288	-0.033	0.011	-0.339	0.341
5	0.350	0.303	0.175	-0.300	0.174	-0.288	-0.040	0.007	-0.337	0.339
6	0.350	0.303	0.175	-0.500	0.178	-0.290	-0.027	0.009	-0.340	0.341
7	0.400	0.346	0.200	-0.100	0.200	-0.335	-0.041	0.006	-0.389	0.392
8	0.400	0.346	0.200	-0.300	0.191	-0.337	-0.051	-0.003	-0.387	0.390
9	0.400	0.346	0.200	-0.500	0.191	-0.337	-0.055	-0.004	-0.387	0.391
10	0.450	0.390	0.225	-0.100	0.221	-0.381	-0.043	0.001	-0.440	0.442
11	0.450	0.390	0.225	-0.300	0.211	-0.383	-0.059	-0.009	-0.437	0.441
12	0.450	0.390	0.225	-0.500	0.213	-0.380	-0.074	-0.005	-0.436	0.442
13	0.500	0.433	0.250	-0.100	0.242	-0.427	-0.048	-0.004	-0.491	0.493
14	0.500	0.433	0.250	-0.300	0.242	-0.424	-0.061	-0.003	-0.488	0.492
15	0.500	0.433	0.250	-0.500	0.238	-0.426	-0.071	-0.007	-0.488	0.493
16	0.550	0.476	0.275	-0.100	0.263	-0.474	-0.049	-0.009	-0.542	0.544
17	0.550	0.476	0.275	-0.300	0.264	-0.469	-0.069	-0.006	-0.538	0.543
18	0.550	0.476	0.275	-0.500	0.264	-0.469	-0.075	-0.006	-0.538	0.543
19	0.600	0.520	0.300	-0.100	0.286	-0.518	-0.054	-0.012	-0.592	0.595
20	0.600	0.520	0.300	-0.300	0.286	-0.515	-0.071	-0.010	-0.589	0.594
21	0.600	0.520	0.300	-0.500	0.291	-0.512	-0.081	-0.004	-0.588	0.594
22	0.650	0.563	0.325	-0.100	0.305	-0.566	-0.054	-0.019	-0.642	0.645
23	0.650	0.563	0.325	-0.300	0.309	-0.561	-0.074	-0.013	-0.640	0.644
24	0.650	0.563	0.325	-0.500	0.312	-0.558	-0.083	-0.008	-0.639	0.645
25	0.700	0.606	0.350	-0.100	0.330	-0.610	-0.058	-0.019	-0.693	0.696

GRID PLANE 5 AZIMUTH ANGLE = 30.00 (continued)

N	R	X	Y	Z	VX	VY	VZ	VR	VT	V
26	0.700	0.606	0.350	-0.300	0.331	-0.606	-0.076	-0.016	-0.691	0.695
27	0.700	0.606	0.350	-0.500	0.334	-0.603	-0.086	-0.012	-0.690	0.695
28	0.750	0.650	0.375	-0.100	0.347	-0.658	-0.057	-0.029	-0.743	0.746
29	0.750	0.650	0.375	-0.300	0.354	-0.651	-0.078	-0.019	-0.741	0.745
30	0.750	0.650	0.375	-0.500	0.348	-0.653	-0.092	-0.025	-0.739	0.746
31	0.800	0.693	0.400	-0.100	0.367	-0.705	-0.054	-0.034	-0.794	0.797
32	0.800	0.693	0.400	-0.300	0.401	-0.682	-0.085	0.006	-0.792	0.796
33	0.800	0.693	0.400	-0.500	0.348	-0.719	-0.041	-0.058	-0.796	0.799
34	0.850	0.736	0.425	-0.100	0.372	-0.758	-0.072	-0.057	-0.843	0.848
35	0.850	0.736	0.425	-0.300	0.454	-0.721	0.000	0.033	-0.851	0.852
36	0.850	0.736	0.425	-0.500	0.417	-0.742	0.004	-0.010	-0.851	0.851
37	0.900	0.779	0.450	-0.100	0.422	-0.796	-0.010	-0.032	-0.900	0.901
38	0.900	0.779	0.450	-0.300	0.451	-0.780	0.010	0.001	-0.901	0.901
39	0.900	0.779	0.450	-0.500	0.448	-0.781	0.005	-0.002	-0.901	0.901
40	0.950	0.823	0.475	-0.100	0.477	-0.824	0.010	0.001	-0.952	0.952
41	0.950	0.823	0.475	-0.300	0.473	-0.825	0.008	-0.002	-0.951	0.951
42	0.950	0.823	0.475	-0.500	0.474	-0.824	0.005	-0.002	-0.951	0.951
43	1.000	0.866	0.500	-0.100	0.497	-0.869	0.018	-0.004	-1.001	1.002
44	1.000	0.866	0.500	-0.300	0.498	-0.868	0.008	-0.003	-1.001	1.001
45	1.000	0.866	0.500	-0.500	0.498	-0.868	0.005	-0.002	-1.001	1.001

GRID PLANE 9 AZIMUTH ANGLE = 60.00

N	R	X	Y	Z	VX	VY	VZ	VR	VT	V
1	0.300	0.150	0.260	-0.100	0.251	-0.139	-0.038	0.006	-0.287	0.290
2	0.300	0.150	0.260	-0.300	0.246	-0.143	-0.042	-0.001	-0.285	0.288
3	0.300	0.150	0.260	-0.500	0.246	-0.143	-0.043	-0.001	-0.285	0.288
4	0.350	0.175	0.303	-0.100	0.298	-0.165	-0.032	0.006	-0.340	0.342
5	0.350	0.175	0.303	-0.300	0.287	-0.178	-0.038	-0.011	-0.337	0.340
6	0.350	0.175	0.303	-0.500	0.287	-0.175	-0.049	-0.008	-0.336	0.340
7	0.400	0.200	0.346	-0.100	0.339	-0.192	-0.049	0.003	-0.389	0.392
8	0.400	0.200	0.346	-0.300	0.333	-0.196	-0.054	-0.003	-0.387	0.390
9	0.400	0.200	0.346	-0.500	0.332	-0.198	-0.058	-0.006	-0.387	0.391
10	0.450	0.225	0.390	-0.100	0.384	-0.216	-0.047	0.005	-0.441	0.443
11	0.450	0.225	0.390	-0.300	0.377	-0.223	-0.059	-0.005	-0.437	0.441
12	0.450	0.225	0.390	-0.500	0.375	-0.224	-0.066	-0.006	-0.437	0.442
13	0.500	0.250	0.433	-0.100	0.423	-0.248	-0.054	-0.003	-0.491	0.494
14	0.500	0.250	0.433	-0.300	0.418	-0.253	-0.061	-0.010	-0.489	0.492
15	0.500	0.250	0.433	-0.500	0.420	-0.247	-0.071	-0.004	-0.488	0.493
16	0.550	0.275	0.476	-0.100	0.466	-0.276	-0.056	-0.006	-0.541	0.544

GRID PLANE 9 AZIMUTH ANGLE = 60.00 (continued)

N	R	X	Y	Z	VX	VY	VZ	VR	VT	V
17	0.550	0.275	0.476	-0.300	0.461	-0.278	-0.071	-0.010	-0.538	0.543
18	0.550	0.275	0.476	-0.500	0.463	-0.275	-0.076	-0.007	-0.538	0.544
19	0.600	0.300	0.520	-0.100	0.507	-0.306	-0.060	-0.011	-0.592	0.595
20	0.600	0.300	0.520	-0.300	0.507	-0.301	-0.072	-0.007	-0.589	0.594
21	0.600	0.300	0.520	-0.500	0.504	-0.303	-0.081	-0.011	-0.588	0.594
22	0.650	0.325	0.563	-0.100	0.548	-0.335	-0.062	-0.016	-0.642	0.645
23	0.650	0.325	0.563	-0.300	0.548	-0.330	-0.077	-0.012	-0.640	0.644
24	0.650	0.325	0.563	-0.500	0.550	-0.326	-0.084	-0.007	-0.639	0.645
25	0.700	0.350	0.606	-0.100	0.590	-0.363	-0.064	-0.020	-0.693	0.696
26	0.700	0.350	0.606	-0.300	0.590	-0.358	-0.080	-0.015	-0.690	0.696
27	0.700	0.350	0.606	-0.500	0.594	-0.351	-0.089	-0.007	-0.689	0.695
28	0.750	0.375	0.650	-0.100	0.631	-0.392	-0.066	-0.024	-0.743	0.746
29	0.750	0.375	0.650	-0.300	0.632	-0.387	-0.083	-0.019	-0.741	0.745
30	0.750	0.375	0.650	-0.500	0.639	-0.371	-0.101	-0.002	-0.739	0.746
31	0.800	0.400	0.693	-0.100	0.672	-0.421	-0.072	-0.028	-0.793	0.796
32	0.800	0.400	0.693	-0.300	0.674	-0.419	-0.066	-0.026	-0.793	0.797
33	0.800	0.400	0.693	-0.500	0.768	-0.261	-0.078	0.158	-0.796	0.815
34	0.850	0.425	0.736	-0.100	0.718	-0.438	-0.100	-0.021	-0.841	0.847
35	0.850	0.425	0.736	-0.300	0.731	-0.432	-0.017	-0.009	-0.849	0.849
36	0.850	0.425	0.736	-0.500	0.739	-0.423	0.013	0.003	-0.852	0.852
37	0.900	0.450	0.779	-0.100	0.815	-0.415	0.101	0.048	-0.913	0.920
38	0.900	0.450	0.779	-0.300	0.780	-0.451	0.003	-0.001	-0.901	0.901
39	0.900	0.450	0.779	-0.500	0.779	-0.452	0.005	-0.001	-0.901	0.901
40	0.950	0.475	0.823	-0.100	0.826	-0.475	0.011	0.002	-0.952	0.952
41	0.950	0.475	0.823	-0.300	0.823	-0.477	0.006	-0.001	-0.951	0.951
42	0.950	0.475	0.823	-0.500	0.822	-0.477	0.005	-0.002	-0.951	0.951
43	1.000	0.500	0.866	-0.100	0.869	-0.499	0.014	0.003	-1.002	1.002
44	1.000	0.500	0.866	-0.300	0.866	-0.502	0.006	-0.002	-1.001	1.001
45	1.000	0.500	0.866	-0.500	0.865	-0.502	0.005	-0.002	-1.001	1.001

APPENDIX B

If the helicopter has a gross weight other than the standard weight used here, a weight correction on the downwash should be added. Based on the momentum theory, the downwash velocity is proportional to the square root of thrust coefficient or the weight for the hover case. Thus, it is assumed that the vertical velocity is proportional to the weight to some power as follows:

$$V_Z' = V_Z * (W_t / GW)^A$$

where,

V_Z' = vertical velocity

V_Z = vertical velocity of standard weight

W_t = helicopter weight

GW= standard weight used to obtain data files, i. e. = 6480 kg.

The exponent A was determined using the wake velocity table compiled by the HOVER code. The natural log of the vertical velocity component and thrust coefficient were plotted and the slopes of the line were obtained as shown in figures B1 and B2. For radial distance of 0.8R or less, the plot shows that the slopes or exponents are similar. The average exponent is A = 0.454 which is close to 0.5 from the momentum theory. For radial distance greater than 0.8, a second order polynomial was used to obtain a equation for exponent A as a function radial distance for C_t less than or equal to 0.008. The exponent for C_t greater than 0.008 are small enough to be ignored. The second order polynomial is

$$A = 13.26 - 31.23 * (r/R) + 19.07 (r/R)^2$$

The velocity at radial distance greater than one radius of blade was not corrected.

APPENDIX C

SUBROUTINE DOWNWASH

The subroutine DOWNWASH will calculate the rotor downwash at a coordinate of interest, of a helicopter in hover. The downwash velocity is calculated by linear interpolations of a set of data files which include downwash velocities, and angular, radial, and vertical ranges files. These files are generated by a potential flow code for rotor in hover(AMI's HOVER code). The angular range is 90 degrees, since the subroutine is written specially for the AH-64 which has four blades. Modification of the "search angle" routine will be required for rotor with other number of blades.

* Outline of the subroutine:

* Coordinate of the subroutine

hub center	origin(0,0,0)
forward(nose)	positive x direction
right	positive y direction
down	positive z direction

* The followings are the required inputs for the subroutine:

VTIP:	Tip velocity (ft/sec)
ANBL:	Number of blades in the main rotor
TIMIN:	Initial Time (sec)
T:	Current Time (sec)
ROTI:	Reference rotor blade angle at time (deg)
RORAD:	Blade radius (ft)
ROTW:	Rotor speed (cycles/sec)
XR,YR,ZR:	Initial rocket position measured from hub center (ft)
LMAX,MMAX,NMAX:	Radial,angular,&vertical upper bounds fo the data range
X,Y,Z:	Current location of the rocket (ft)

* The followings are athe required input files from rotor code:

Q.OUT:	Downwash velocity file(Velocity is given at each.of the Z levels at every radial increment of each angular increment.)
TR.OUT:	Radial increments file
TZ.OUT:	Vertical increments file(negative down)
TA.OUT:	Angular increments file(phi=0 deg on vertical axis)

* Create the TA(M), TR(L), TZ(N), TVWZ(L,M,N) files for the subroutine

TVWZ(L,M,N):	Downwash velocity file where L = radial,
	M = angular,
	N = vertical(positive down)
TR(L):	Radial range
TA(M):	Angular range
TZ(N):	Vertical range

* Calculate reference rotor blade angle

CYCS:	Number for cycles travelled by the the reference blade
ROTANG:	Total ref. blade angle, converted to a (0-360deg) range

* Calculate radial position of rocket for a given positions:

Initial: (XR,YR,ZR)

Current: (X,Y,Z)

R = SQRT((XR + X)**2. + (YR + Y)**2.) / RORAD

The radial distance is normalized by the rotor radius.

* Calculate the angle of the first blade beyond phi = 0 deg(tail)

BLSP:	Blade spacing
RII:	Number of "whole" blade w/in the ref. blade angle, ROTANG RANG: Angle of the first blade beyond phi = 0 deg(tail)

RANG is calculated to find the angle of the second blade (RANG + 90deg) beyond phi=0deg, which is used to find the search angle.

* Calculate the angle fo the rocket, MANG

MANG = ATAN((XR+X)/(YR+Y)) + 90

The rocket angle is measured from phi=0 deg(helicopter tail).

* Calculate the search angle, A

The difference, (RANG+90) - MANG, is used to determine whether the rocket is infront, below, or behind the second blade beyond the tail.

If the difference is:

*(negative) - The rocket is infront of the blade and

A = 90 - (MANG - (RANG + 90))

*(zero) - The rocket is below the the blade and

A = 0

*(positive) - The rocket is behind the blade and

A = (RANG + 90) - MANG

The search angle is calculated in accordance with the angular range format where zero deg is on the vertical axis and 90 deg is on the horizontal axis. The angular range occupies the first quadrant.

* Search for radial, angular, and vertical index from the range files and calculate the ratios for interpolation of the velocity file

The velocity file is in cyclindrical form. The search routine is the same for the three coordinates. It will step through the data file until a value greater than the search value(angle, radius, or z) is found. Interpolation is done linearly between two nearest values.

Example:

IF (TR(1) .LT. R) GOTO 1005

-Since R, the search value, is greater than the first value, continue to step through the data file TR(L).

-If the search value is less than the TR(1),

L = 2	The search index for radial range is 2.
RATO1 = 0.0	The first radial value is used.
GOTO 1010	Go to the next search routine.

```
1005        DO 1020 L = 2, LMAX
            IF (TR(L) - R) 1020, 1025, 1030
1020        CONTINUE
```

The above DO loop step through the TR(L) file; if TR(L) - R is negative, it'll continue to search.

if TR(L) - R is zero(equal), the ratio is one and go to the next search routine.

```
1025        RATO1 = 1.0
            GOTO 1010
```

if TR(L) - R is positive, calculate the ratio linearly, and go to the next search.

```
1030    RATO1 = (R-TR(L-1)) / (TR(L)-TR(L-1))
```

* Interpolate linearly

Interpolations are done in the radial-angular plane at two Z levels. It is first interpolated in the radial direction with TOP1 AND TMP1 and then in the angular direction with DELVZ1. This is done similarly in the second, lower Z level.

* Calculate downwash

The downwash velocity is calculated by a final interpolation in the Z direction and a convertion to the physical space with the tip velocity.

```
\newpage
c   ****************************************
c   ***program to test downwash subroutine***
c
      real x,y,z,timin,t,vwze,vwre,ba,mang,rotang
      real xx(20),time(20),u,gw,wt
      integer i,j,k,l,m,n
c
c   ****The upper bounds of R, Angle, & Z****
      data l,m,n/37,13,25/
c   ****Sample t & x data****
      data (time(i),i=1,13)/.092,.0953,.0995,.1068,.1215,
     *        .1459,.1704,.1847,.1915,.2033,.2152,.2359,.2670/
      data (xx(k),k=1,13)/.109,.848,1.744,3.733,7.633,12.268,
     *     15.329,16.86,19.677,22.667,28.315,37.78,48.441/
      data u/15./
      gw = 14463.
      wt = 16463.
      open(1,file='outputs',status='new')
c   ***Setting z = zr, y = yr, & inital t***
      z = 6.71
      y = 0.0
      timin = 0.092
c   ****Creating output table with ah64downwash subroutine****
      write(1,*) 'Apache in Hover'
      write(1,80) u
      write(1,90) gw,wt
      write(1,100)
      write(1,150)
      write(1,155)
      write(1,205)
      write(1,*)
      do 30 k =  1, 13
      x = xx(k)
      t = time(k)
      call ah64downwash(u,timin,t,wt,x,y,z,ba,rotang,vwze,vwre,vwte)
      write(1,200) t,x,rotang,vwre,vwte,vwze
30  continue
80  format('Vehicle Velocity(ft/sec): Vx = ',f8.2)
90  format('Ref Weight(lbs) = ',f8.1,3x,'Actual Weight(lbs) = ',f8.1)
100     format('Z = 6.71ft',5x,'timin = 0.092sec',5x,'anbl = 4')
150     format('roti = 0.0',5x,'rotw = 4.8078c/s',5x,'rorad = 24ft')
155     format('xr = -0.31ft',3x,'yr = 8.17ft',10x,'zr = 6.71ft')
200     format(f6.3,2x,f7.3,2x,f11.3,6x,f8.3,5x,f7.2,6x,f7.2)
205     format('T(sec)',3x'X(ft)',2x,'Ref Rotor Angle',2x,
     *    'Vr(ft/sec)',3x,'Vt(ft/sec)',3x,'Vz(ft/sec)')
```

```
      close(1)
      end

C

c

      SUBROUTINE
AH64DOWNWASH(U,TIMIN,T,WT,X,Y,Z,A,ROTANG,VWZE,VWRE,VWTE)

C

c     **This subroutine calculate the downwash,vwze,Vr,&Vt(ft/s) at a given
c     coordinate(x,y,z), feet, from the launcher position(xr,yr,zr),feet,
c     which is measured from the rotor hub center, and a time,t(sec), from
c     the initial time, timin(sec).
c
c     ANBL:     NUMBER OF BLADES IN MAIN ROTOR
C     ROTI: REFERENCE ROTOR BLADE ANGLE AT TIMIN, DEG
C     ROTW:     ROTOR SPEED, CYCLES/SEC
C     RORAD:  ROTOR RADIUS, FT
C     GW:    GROSS WEIGHT, LBS, USED IN DATA FILES CALCULATION
C     WT:    HELICOPTER WEIGHT, LBS
C     SIGMA:    ROTOR SOLIDITY
C     CD:    MEAN ROTOR DRAG COEFFICIENT
C     TIMIN:    TIME AT WHICH CALCULATION STARTS, SEC
c     U: HELICOPTER VELOCITY IN X DIRECTION, FT/SEC
C     XR,YR,ZR:    INITIAL POSITIONS OF ROCKET ON LAUNCHER MEASURED
C              FROM ROTOR HUB CENTER, FT
c     lmax,mmax,nmax:      radial,angular,vertical upper bounds(integers)
c     vtip:          tip velocity(ft/sec)
c     num:           total number of velocities calculated
c     q.out:         downwash velocity file for interpolation
c     tr.out:        radial increments file for interpolaton
c     ta.out:        angular increments file for interpolation
c     tz.out:        vertical increments file for interpolation
c
      real a, anbl, blsp, cycs,delvz1,delvz2,top2,tmp1
      real r, rang, rato1,rii,rorad,roti,rotw,rotang
      real t,ta(90),timin,tmp2,top1,tr(90),tvwz(90,90,9)
      real x,xr,yr,zr,vwze,MANG,y,z,tvwr(90,90,9),gw,cd,pi
      real lmax, mmax, nmax,num,tz(9),vwre,rho,sigma,wt,ct
      real rato3,rato2,ztemp(4000),vtip,rtemp(4000)
      real vtp,vti,vwte,slope,u,wang,kx,g,vo,voh
      integer ii, l, m,n,i,k,j
C
```

```
c   ***data***
c   These data a particular to the AH-64 and Lmax, Mmax & Nmax
c   are the upper bounds of the radial, angular, and vertical
c   data files respectively. They can be passed into the subroutine.
c
    data gw/14436./
    data vtip /725./
    data anbl /4./
    data roti /0.0/
    data rotw /4.80783333/
    data rorad /24.0/
    data sigma/0.092/
    data cd /0.01/
    data rho /0.0023769/
    data xr,yr,zr/-0.31,8.17,6.71/
    data lmax, mmax, nmax/37,13,3/
c   data wt /16436.0/
    data pi /3.14159265/
c
c   *****Create ta, tr, tz, tvxz files*****
c   Using the coresponding output files from a potential flow
c   lifting surface code for rotors in hover or climb(J.M. Summa)
c
    open(77,file='q.out',status='old')
    open(78,file='tr.out',status='old')
    open(79,file='ta.out',status='old')
    open(80,file='tz.out',status='old')
c
    num = lmax*mmax*nmax
c   read(77,*) (temp(i),i=1,num)
    do 15 i = 1, num
        read(77,3000) ztemp(i), rtemp(i)
15  continue
    i=0
    do 20 m=1,mmax
        do 25 l=1,lmax
            do 30 n=1,nmax
            i=i+1
            tvwr(l,m,n) = rtemp(i)
30          tvwz(l,m,n) = ztemp(i)
25      continue
20  continue
    read(78,*) (tr(l),l=1,lmax)
    read(79,*) (ta(m),M=1,mmax)
    read(80,*) (tz(n),n=1,nmax)
c   ****Z is positive down in the subroutine***
```

```
      do 10 i = 1,nmax
10    tz(i) = -1.*tz(i)
c
C     *******This calculation should be done at each (x z t)*******
c                 where downwash is need.
c
c     *****calculate reference rotor blade angle*****
c
      CYCS = ROTW * (T - TIMIN)
      ROTANG = ROTI + 360. * (CYCS - INT(CYCS))
      ROTANG = AMOD(ROTANG, 360.)
C
c     ***CALCULATE RADIAL POSITION OF MISSILE***
C
      R = SQRT((YR+Y)**2.+(XR+X)**2.)/RORAD
C
C     CALCULATE ANGULAR POSITION OF THE FIRST BLADE FROM PHI=0.0
C
      BLSP = 360. / ANBL
      II = ROTANG/BLSP
      RII = II
      RANG = ROTANG-RII*BLSP
C
c     CALCULATE ANGULAR POSITION OF THE MISSILE FROM PHI=0.0
C
      MANG = ATAN((XR+X)/ABS(YR+Y))
      MANG = MANG*180./3.14159265359 + 90.
C
C     CALCULATE SEARCH ANGLE IN DATA MATRIX
C
      IF (RANG + BLSP - MANG) 100, 200, 300
100     A = BLSP-(MANG -RANG - BLSP)
      goto 400
200     A = 0.0
      goto 400
300     A = RANG + BLSP - MANG
C
C     SEARCH RADIAL TABLE FOR R POSITION
c     AND CALCULATE THE RATIO FOR INTERPOLATION
C
400     IF (TR(1) .LT. R) GOTO 1005
      L = 2
      RATO1 = 0.0
      GOTO 1010
1005    DO 1020 L = 2, LMAX
      IF (TR(L) - R) 1020,1025,1030
```

```
1020   CONTINUE
1025   RATO1 = 1.0
       GOTO 1010
1030   RATO1=(R-TR(L-1))/(TR(L)-TR(L-1))
C
C  SEARCH ANGLE TABLE FOR 'A' POSITION
c  AND CALCULATE THE RATIO FOR INTERPOLATION
C
1010   IF (TA(1) .LT. A) GOTO 1035
       M = 2
       RATO2 = 0.0
       GOTO 1040
1035   DO 1050 M = 2, MMAX
       IF (TA(M) -A) 1050, 1055,1060
1050   CONTINUE
1055   RATO2 = 1.0
       GOTO 1040
1060   RATO2 = (A-TA(M-1))/(TA(M)-TA(M-1))
C
c  SEARCH Z TABLE FOR Z POSITION
c  AND CALCULATE THE RATIO FOR INTERPOLATION
C
1040   IF (TZ(1) .LT. Z/rorad) GOTO 1065
       N = 2
       RATO3 = 0.0
       GOTO 1070
1065   DO 1080 N = 2, NMAX
       IF (TZ(N)-Z/rorad) 1080,1085,1090
1080   CONTINUE
1085   RATO3 = 1.0
       GOTO 1070
1090   RATO3=(Z/rorad-TZ(N-1))/(TZ(N)-TZ(N-1))
c
C  INTERPOLATE LINEARLY ON R, ANGLE, and Z
c  Interpolation is done at z-1 and z levels for radial and angular
c  positions, and finally, between the z levels.
C
1070   TOP1=TVWZ(L-1,M-1,N-1)+RATO1*(TVWZ(L,M-1,N-1)-TVWZ(L-1,M-1,N-1))
       TMP1=TVWZ(L-1,M,N-1)+RATO1*(TVWZ(L,M,N-1)-TVWZ(L-1,M,N-1))
       DELVZ1=TOP1+RATO2*(TMP1-TOP1)
c
       TOP2=TVWZ(L-1,M-1,N)+RATO1*(TVWZ(L,M-1,N)-TVWZ(L-1,M-1,N))
       TMP2=TVWZ(L-1,M,N)+RATO1*(TVWZ(L,M,N)-TVWZ(L-1,M,N))
       DELVZ2=TOP2+RATO2*(TMP2-TOP2)
C
C  CALCULATE AVERAGE DOWNWASH (multiple by Vtip)
```

```
C
      VWZE = (DELVZ1 + RATO3*(DELVZ2-DELVZ1))*vtip
c
c     ****Repeat Interpolations and calc. radial vel****
c
      TOP1=TVWR(L-1,M-1,N-1)+RATO1*(TVWR(L,M-1,N-1)-TVWR(L-1,M-1,N-1))
      TMP1=TVWR(L-1,M,N-1)+RATO1*(TVWR(L,M,N-1)-TVWR(L-1,M,N-1))
      DELVZ1=TOP1+RATO2*(TMP1-TOP1)
c
      TOP2=TVWR(L-1,M-1,N)+RATO1*(TVWR(L,M-1,N)-TVWR(L-1,M-1,N))
      TMP2=TVWR(L-1,M,N)+RATO1*(TVWR(L,M,N)-TVWR(L-1,M,N))
      DELVZ2=TOP2+RATO2*(TMP2-TOP2)
C
C     CALCULATE AVERAGE RADIAL VELOCITY (multiple by Vtip)
C
      VWRE = (DELVZ1 + RATO3*(DELVZ2-DELVZ1))*VTIP
C
c     **Adjust Vz,Vr for weight(WT) other than weight(GW)**
c
      IF (R .LE. 0.8) THEN
          VWZE = VWZE*(WT/GW)**0.454
          VWRE = VWRE*(WT/GW)**0.454
      ENDIF
      IF (CT .LE. 0.008) THEN
         IF (R .GT. 0.8 .AND. R .LE. 1.) THEN
         SLOPE = 13.261-31.234*R+19.067*R*R
         VWZE = VWZE*(WT/GW)**SLOPE
         ENDIF
      ENDIF
c
c     **Calculate tangential velocity as the sum of profile and induced V's**
c
      CT = WT/(PI*RHO*(RORAD*VTIP)**2.)
      VTP = -SIGMA*CD*0.25*2./SQRT(CT)*R
      VTI = -(R/SQRT(CT/2.))*(1.-SQRT(1.-2.*CT/(R*R)))*VWZE/VTIP
c
c     **when (2*Ct/(R*R)) is greater than 1, VTI will be undefine**
c      so it is set to zero.
c
      IF (2.*CT/(R*R) .GT. 1.) VTI = 0.0
      VWTE = -VTIP*(VTI+VTP)
C
c     ***********Correction for low speed forward flight***************
      if (u .eq. 0.) goto 1100
c     ** Calculate the momentum induced velocity, VOH, for hovering **
c              and low speed flight
```

```
c
      VOH = SQRT(WT/(2.*RHO*PI*R*R))
      VO = SQRT(.5*(-U*U+SQRT(U**4. + 4.*VOH**4.)))
C
c     *** Calculate the skew angle of the rotor wake **
c     slope of the inflow gradient & the longitudinal inflow gradient
c
      WANG = ATAN(U/VO)
      KX = TAN(WANG/2.)
      G = 1.+KX*R*COS(MANG + PI/2.)
c
c     ** Correct the velocity components(includes vehicle velocity compo.) **
c
      ANGLE = ATAN2((XR+X),(YR+Y))
      VWZE = VWZE*G*VO/VOH
      VWTE = -G*VTIP*(VTI*VO/VOH+VTP)-U*COS(ANGLE)
      VWRE = VWRE - U*SIN(ANGLE)
C
3000  format (f10.3,f10.3)
1100  CLOSE(77)
      CLOSE(78)
      CLOSE(79)
      CLOSE(80)
      RETURN
      END
```

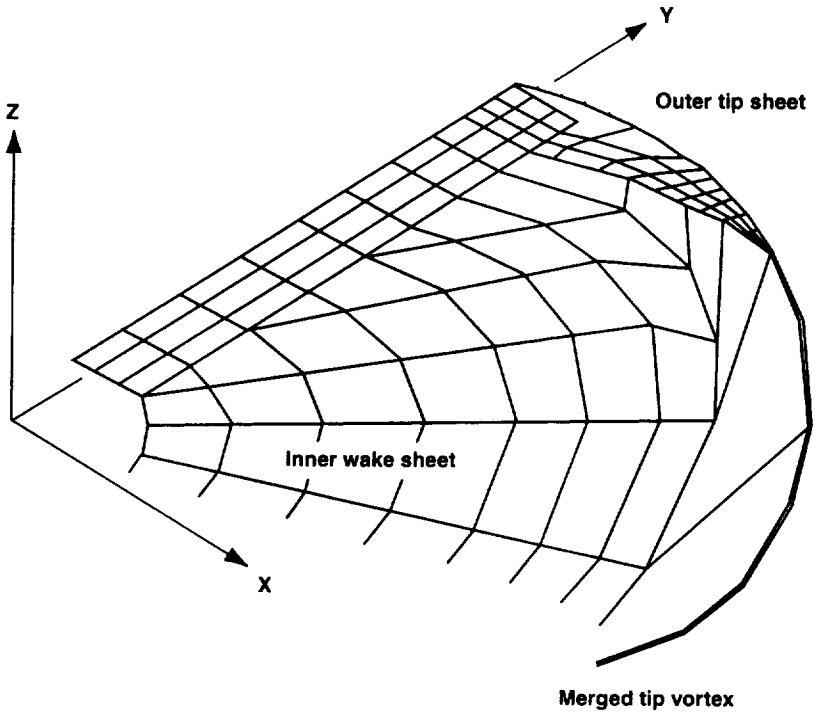

Figure 1. Rotor Blade Vortex Lattice Model.

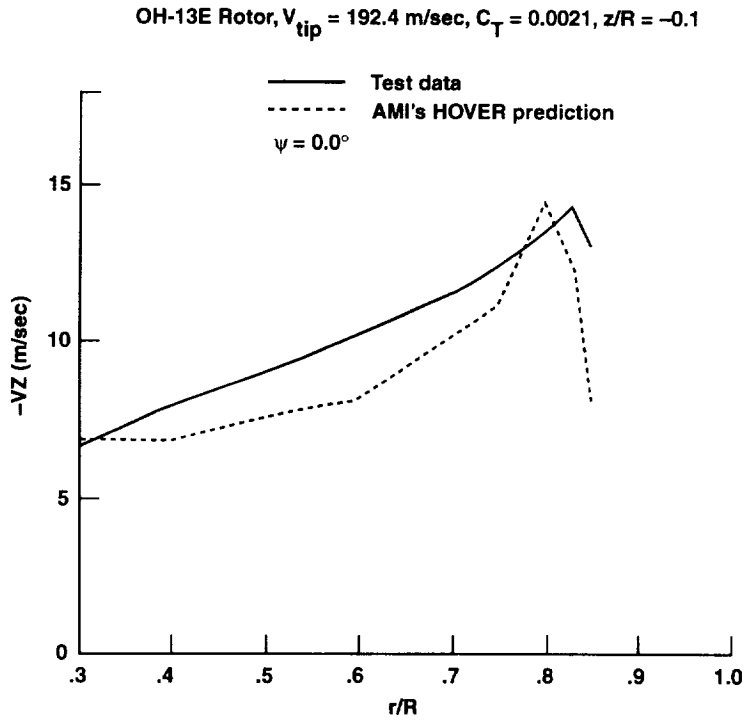

Figure 2(a). Predicted and measured vertical velocity components in wake of OH-13E rotor, $\psi = 0.0°$.

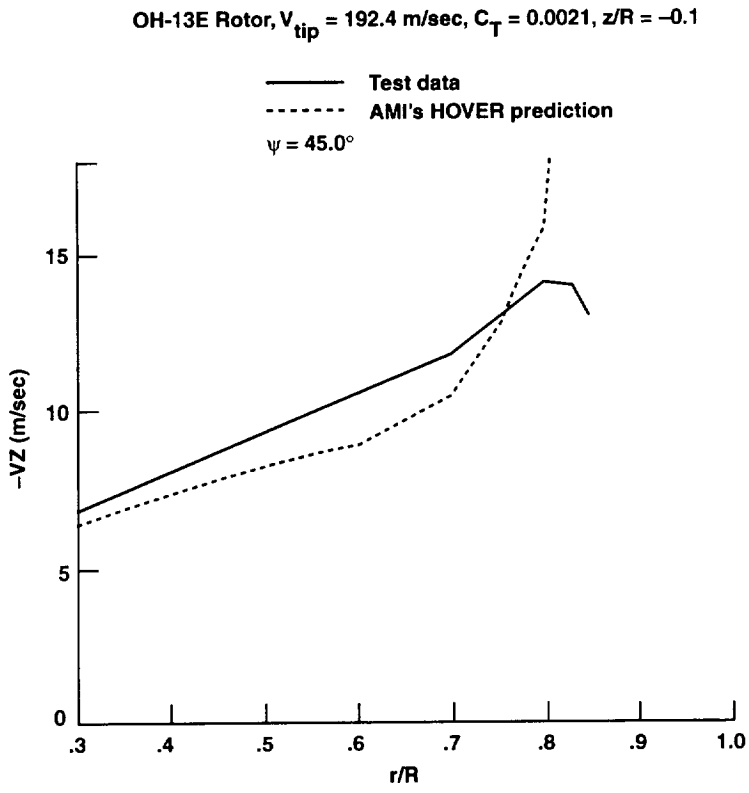

Figure 2(b). Predicted and measured vertical velocity components in wake of OH-13E rotor, ψ = 45°.

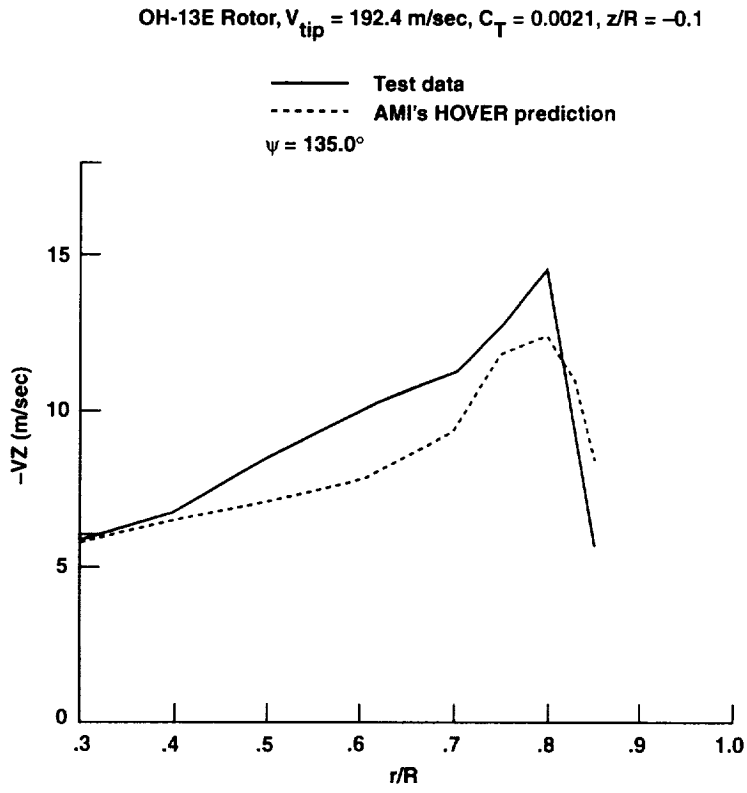

Figure 2(c). Predicted and measured vertical velocity components in wake of OH-13E rotor, ψ = 90°.

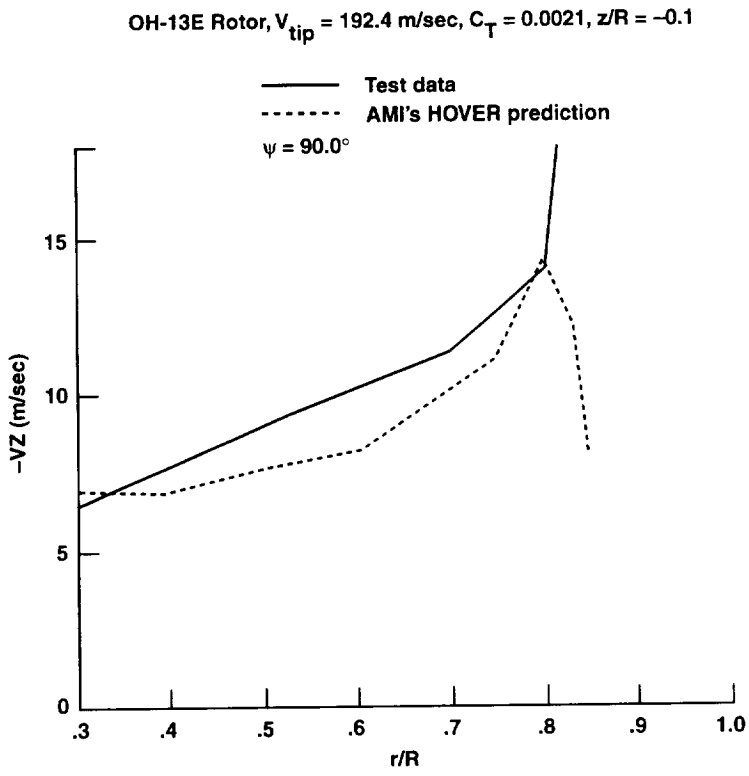

Figure 2(d). Predicted and measured vertical velocity components in wake of OH-13E rotor, $\psi = 135°$.

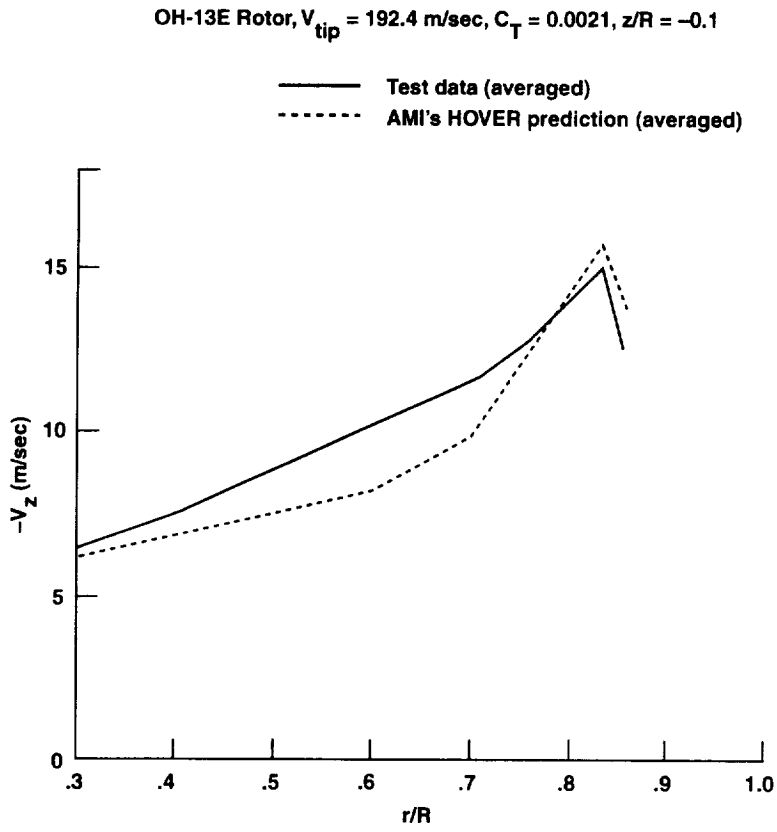

Figure 3. Comparison of predicted mean values with measurements for the test conditions.

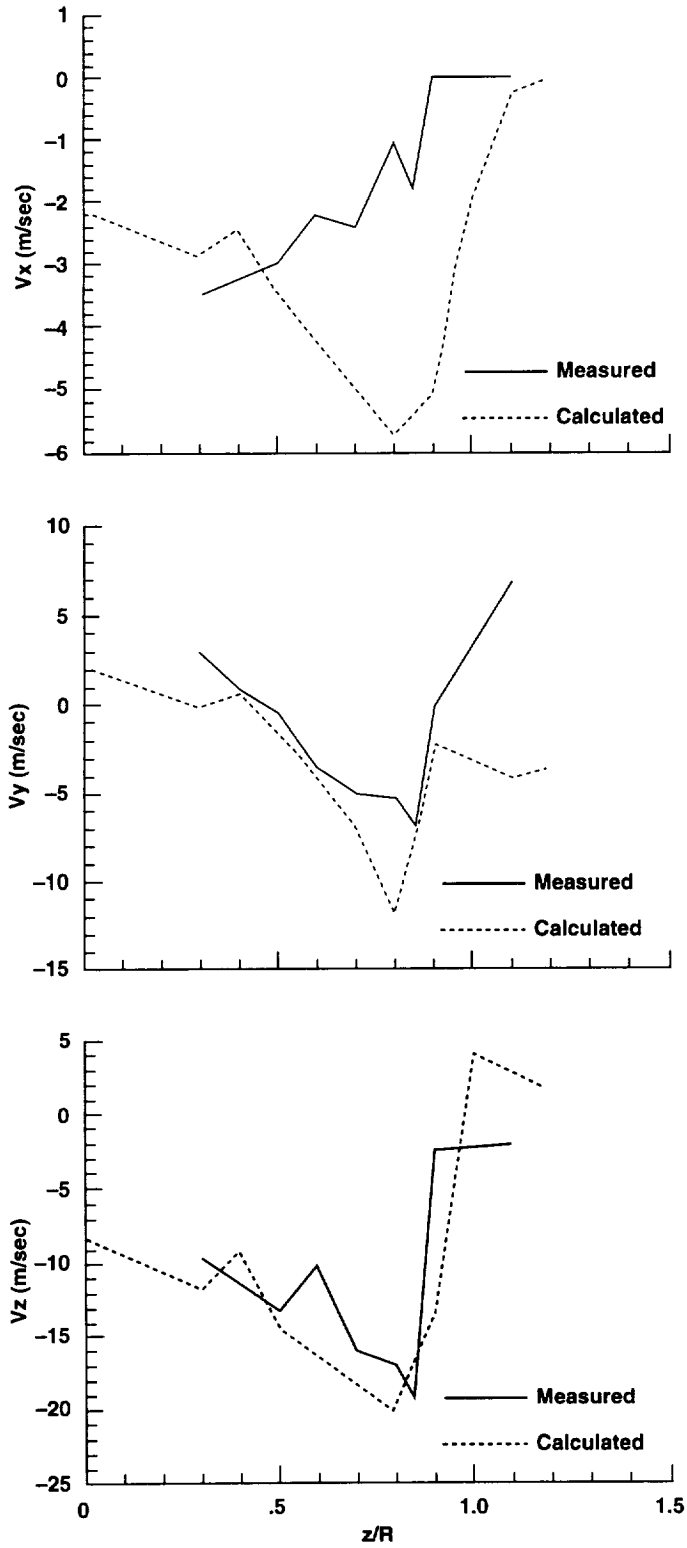

Figure 4. Comparisons of measured and predicted velocity data with a 4-bladed hingeless model rotor, $z/R = -0.07$.

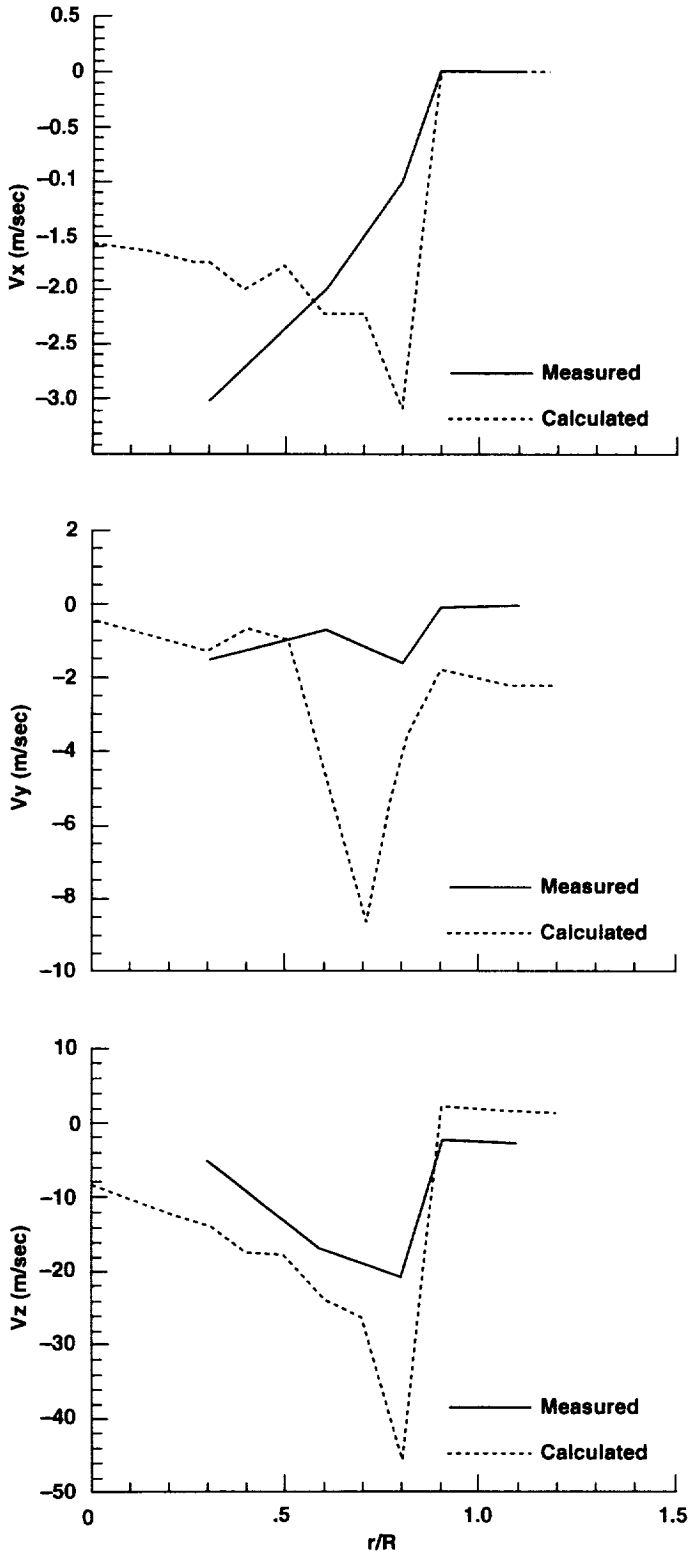

Figure 5. Comparison of measured and predicted velocity data with a 4-bladed model hingeless rotor, $r/R = -.3$.

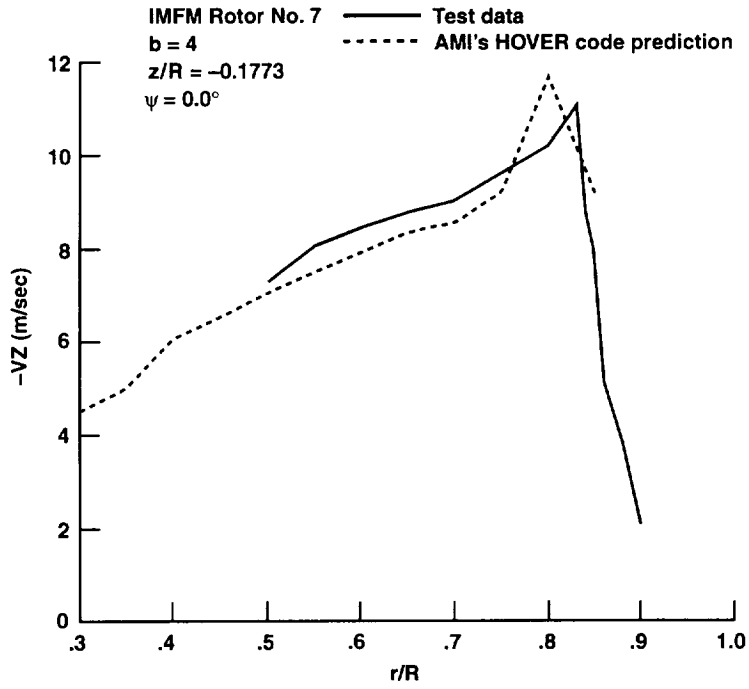

Figure 6(a). Comparison of measured and predicted vertical velocity components in the wake of a 4-bladed model rotor, $\psi = 0.0°$.

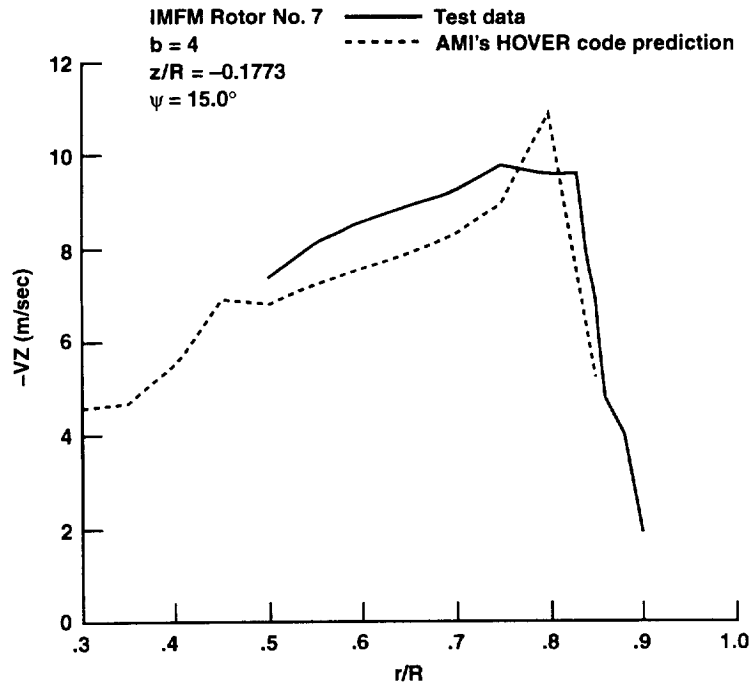

Figure 6(b). Comparison of measured and predicted vertical velocity components in the wake of a 4-bladed model rotor, $\psi = 15.0°$.

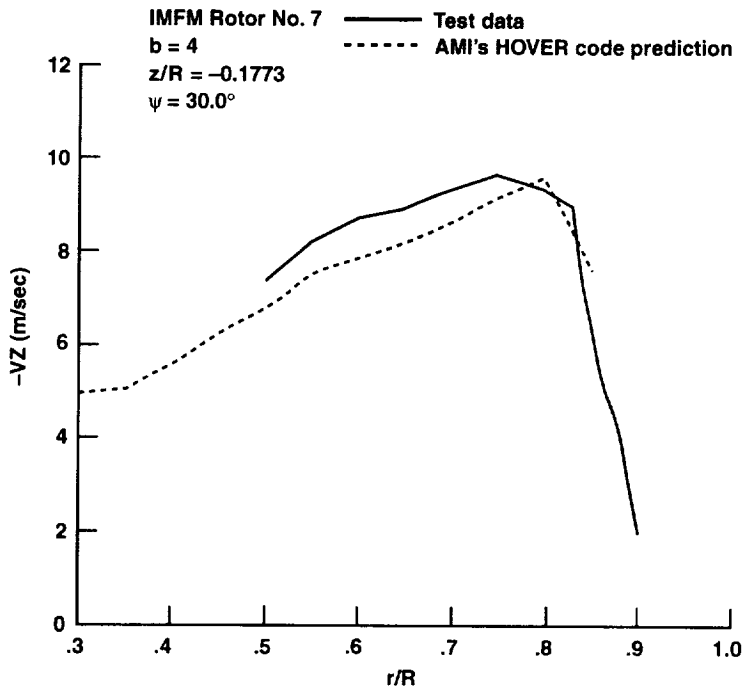

Figure 6(c). Comparison of measured and predicted vertical velocity components in the wake of a 4-bladed model rotor, $\psi = 30.0°$.

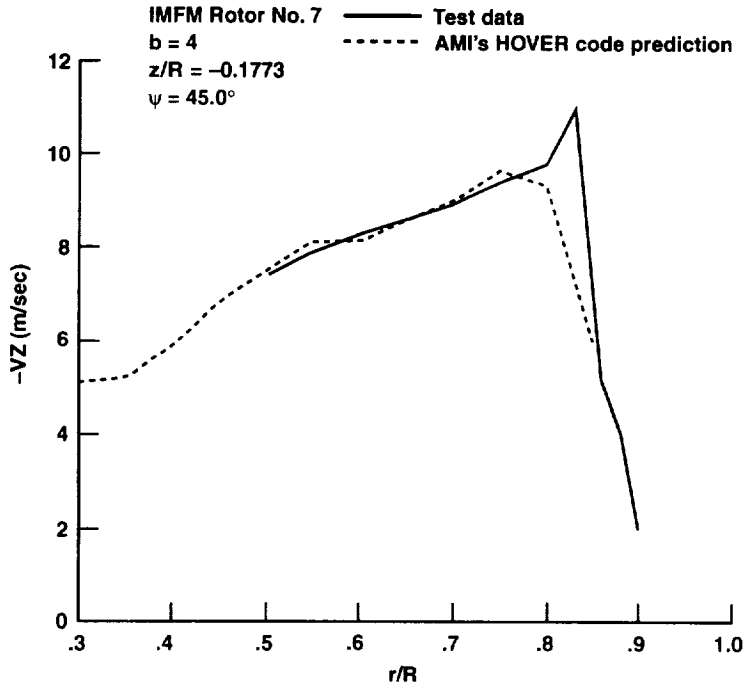

Figure 6(d). Comparison of measured and predicted vertical velocity components in the wake of a 4-bladed model rotor, $\psi = 45.0°$.

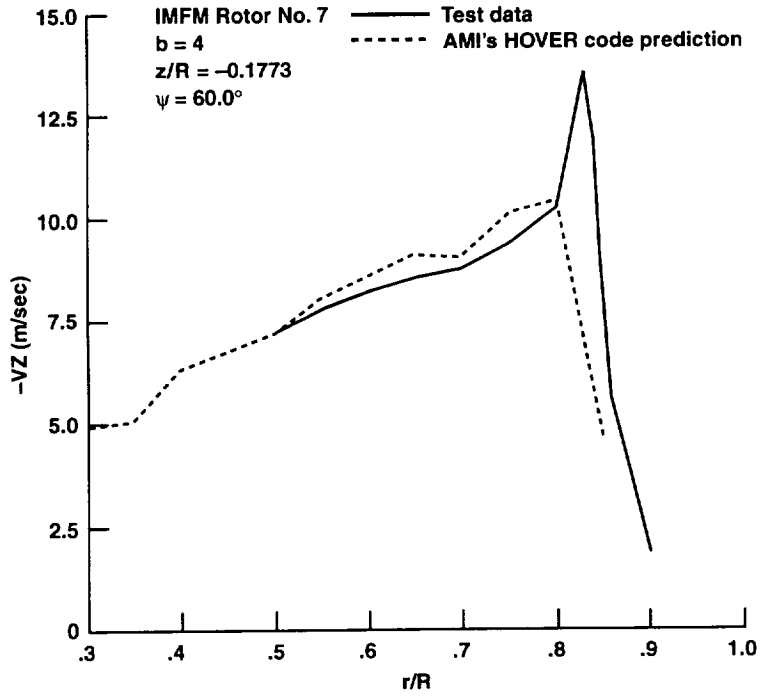

Figure 6(e). Comparison of measured and predicted vertical velocity components in the wake of a 4-bladed model rotor, $\psi = 60.0°$.

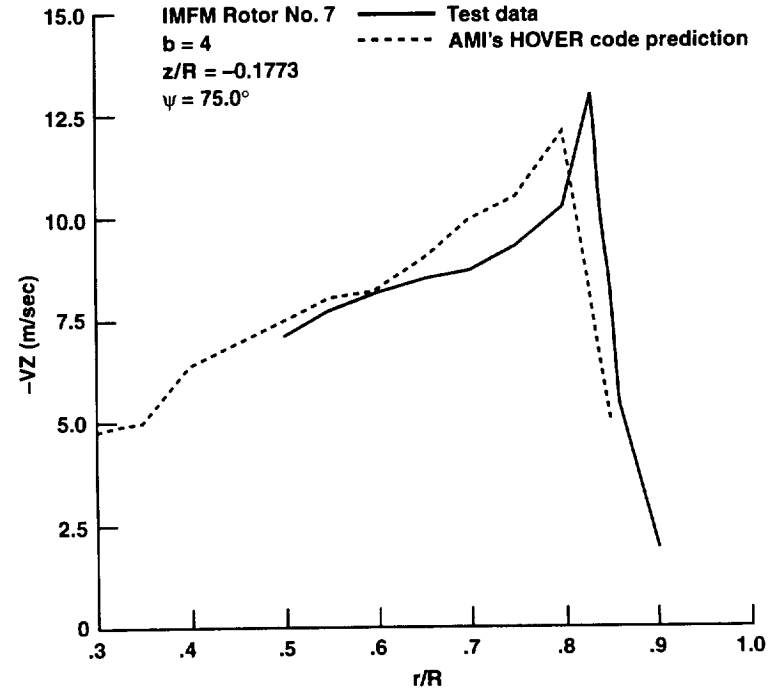

Figure 6(f). Comparison of measured and predicted vertical velocity components in the wake of a 4-bladed model rotor, $\psi = 75.0°$.

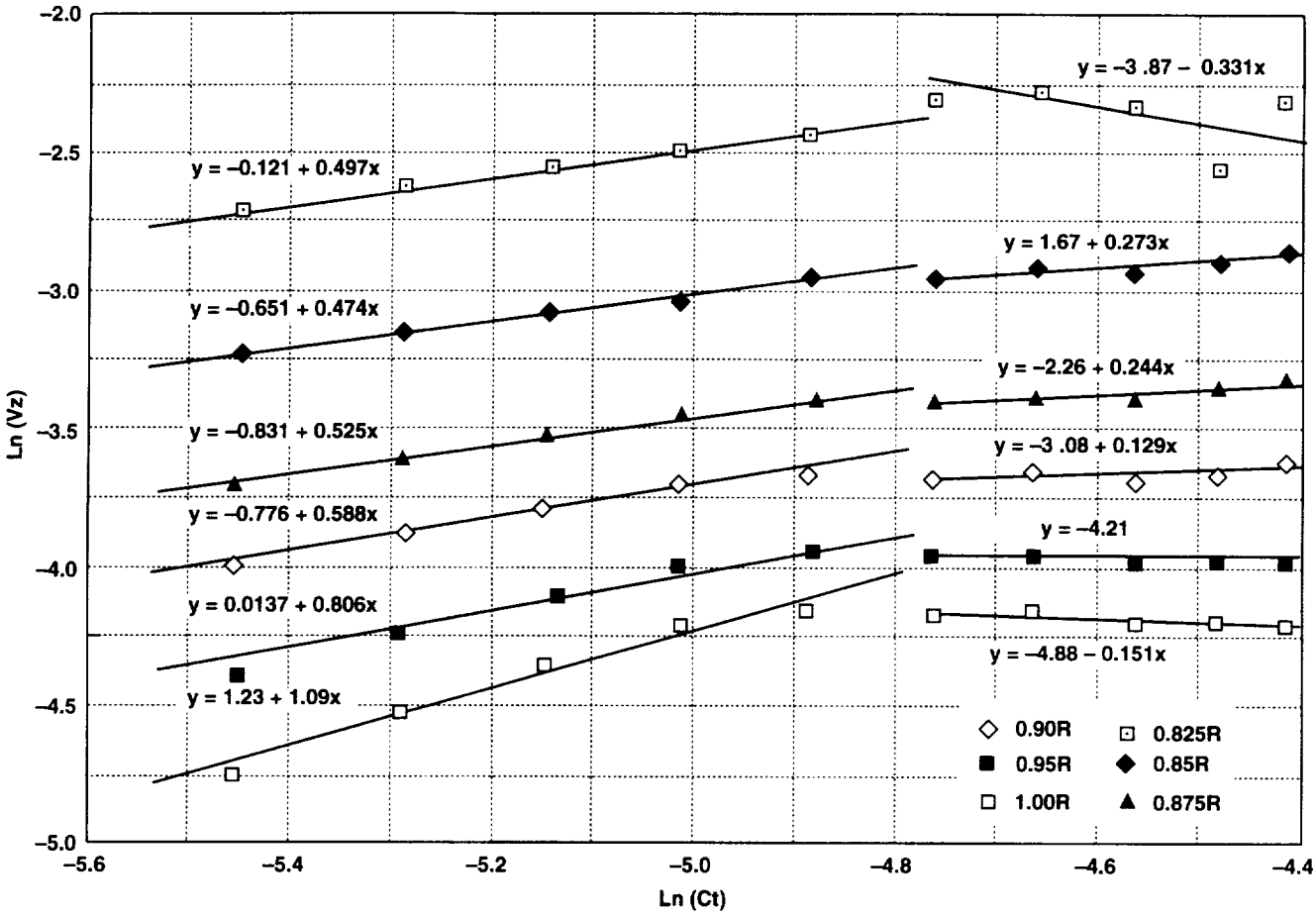

Figure B1. Ln(Vz) vs Ln(Ct) at Various Radial Stations.

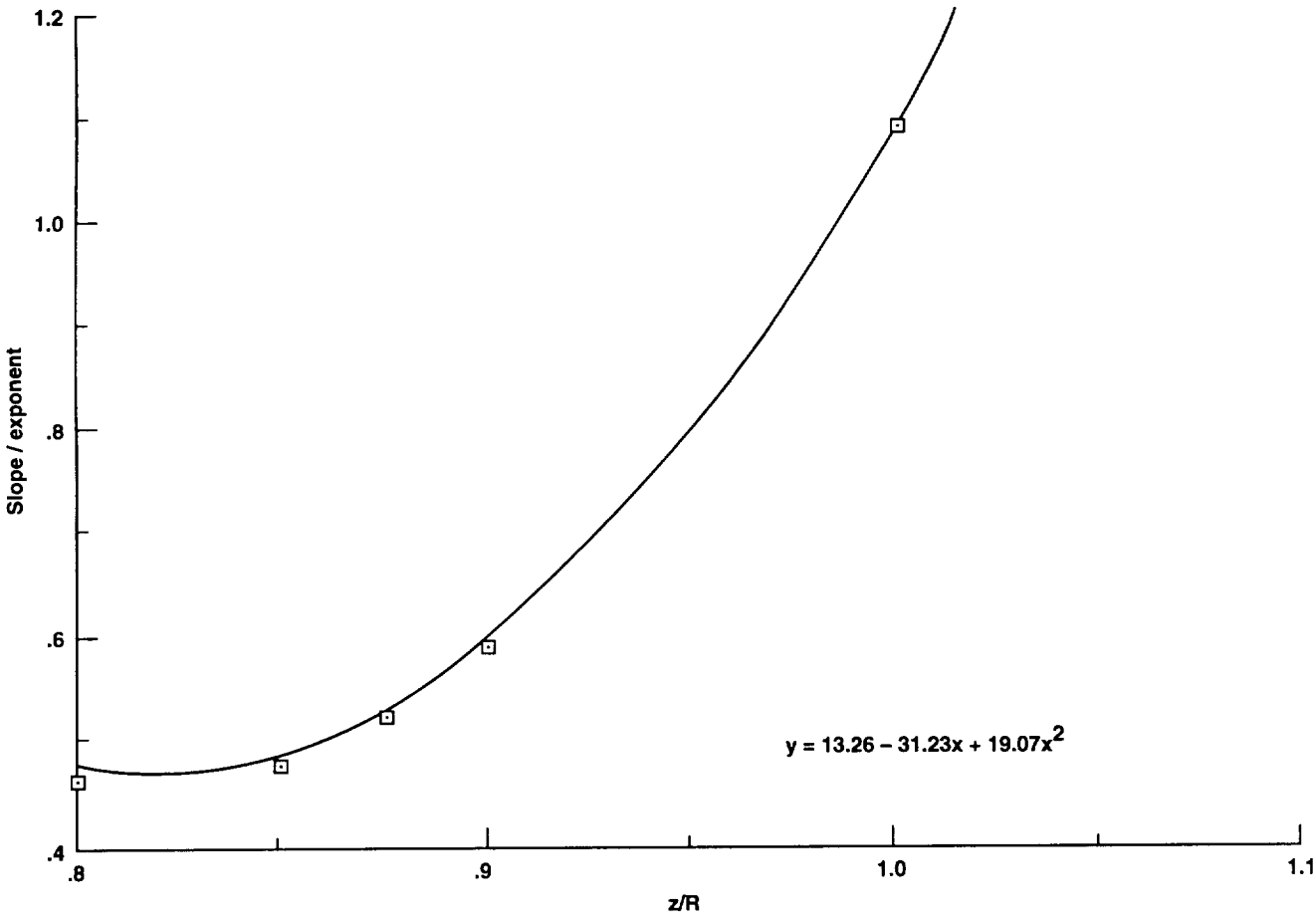

Figure B2. Empirical equation of exponent as function of radial location.

REPORT DOCUMENTATION PAGE

Form Approved
OMB No. 0704-0188

1. AGENCY USE ONLY *(Leave blank)*	2. REPORT DATE	3. REPORT TYPE AND DATES COVERED
	February 1997	Technical Memorandum

4. TITLE AND SUBTITLE

Flow Field Around a Hovering Rotor

5. FUNDING NUMBERS

505-59-87

6. AUTHOR(S)

C. Tung and S. Low

7. PERFORMING ORGANIZATION NAME(S) AND ADDRESS(ES)

Aeroflightdynamics Directorate, U.S. Army Aviation and Troop Command, Ames Research Center, Moffett Field, CA 94035-1000

8. PERFORMING ORGANIZATION REPORT NUMBER

A-975370

9. SPONSORING/MONITORING AGENCY NAME(S) AND ADDRESS(ES)

National Aeronautics and Space Administration
Washington, DC 20546-0001 and U.S. Army Aviation and Troop Command, St. Louis, MO 63120-1798

10. SPONSORING/MONITORING AGENCY REPORT NUMBER

NASA TM-110426
USAATCOM TR-96-A-012

11. SUPPLEMENTARY NOTES

Point of Contact: C. Tung, Ames Research Center, MS 215-A, Moffett Field, CA 94035-1000
(415) 604-5241

12a. DISTRIBUTION/AVAILABILITY STATEMENT

Unclassified-Critical Technology—Distribution limited to U.S. Government agencies and their contractors. Other requests shall be referred to the Aeroflightdynamics Directorate, U.S. Army ATCOM, Ames Research Center, Moffett Field, CA 94035-1000.
Subject Category – 02

Available from the NASA Center for AeroSpace Information,
800 Elkridge Landing Road, Linthicum Heights, MD 21090; (301) 621-0390

12b. DISTRIBUTION CODE

13. ABSTRACT ***(Maximum 200 words)***

A lifting surface hover code developed by the Analytical Method Inc. (AMI) was used to compute the average and unsteady velocity flow field of an isolated rotor without ground effect. The predicted velocity field compares well with experimental data obtained by hot-wire anemometry and by Laser Doppler Velocimetry. A subroutine "DOWNWASH" was written to predict the velocity field at any given point in the wake for a given blade position.

14. SUBJECT TERMS	15. NUMBER OF PAGES
Rotor wake, Downwash velocity, Hovering Rotor	42
	16. PRICE CODE: A03

17. SECURITY CLASSIFICATION OF REPORT	18. SECURITY CLASSIFICATION OF THIS PAGE	19. SECURITY CLASSIFICATION OF ABSTRACT	20. LIMITATION OF ABSTRACT
Unclassified	Unclassified		